

## **Supporting Information**

### Experimental:

#### *Preparation of bulk VO<sub>2</sub>(B):*

VO<sub>2</sub>(B) was prepared from NH<sub>4</sub>VO<sub>3</sub> (Aldrich) solution dissolved in oxalic acid by hydrothermal technique similar to previously reported by Xie and the co-workers.<sup>1</sup> In typical procedure 1 mmol of NH<sub>4</sub>VO<sub>3</sub> was dissolved in 15 ml of deionized water, then 1 M oxalic acid (Aldrich) was added dropwise until pH 1.3. The mixture was then placed in a 23 ml Teflon lined autoclave with stainless steel shell and kept for 1 day at 200 °C. After cooling down to room temperature the product was washed with deionized water and pure ethanol at least three times to remove any impurities. Finally, the VO<sub>2</sub>(B) was dried in air at 60 °C for 2-3 h.

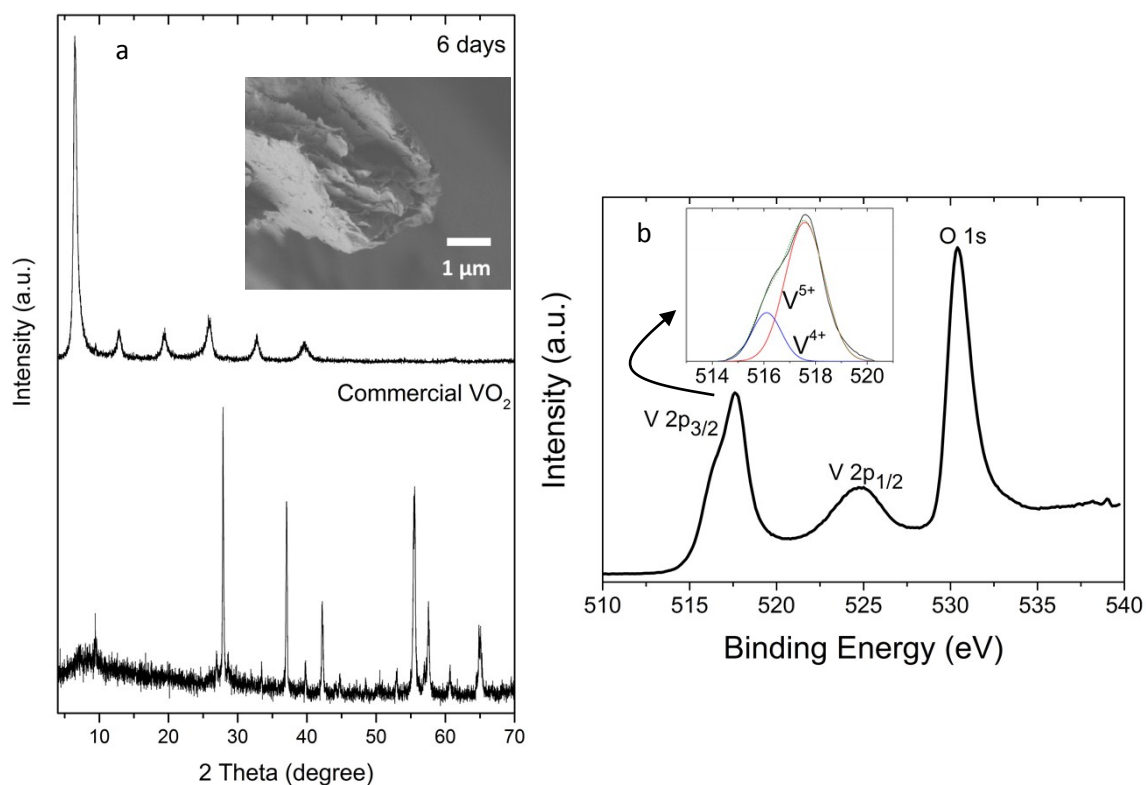


Figure S1: (a) Powder XRD patterns for commercial VO<sub>2</sub> (which matches well with the standard pattern for VO<sub>2</sub>(M), (JCPDS No. 082-0661)), compared with that after 6 days of reflux in water at 60 °C; inset in (a) shows the SEM image of the exfoliated V<sub>2</sub>O<sub>5</sub>·nH<sub>2</sub>O material obtained from VO<sub>2</sub>(M) after 6 days of reflux. (b) XPS spectrum for V<sub>2</sub>O<sub>5</sub>·0.55H<sub>2</sub>O nanosheets; inset in (b) shows the deconvolution of V 2p<sub>3/2</sub> peak.

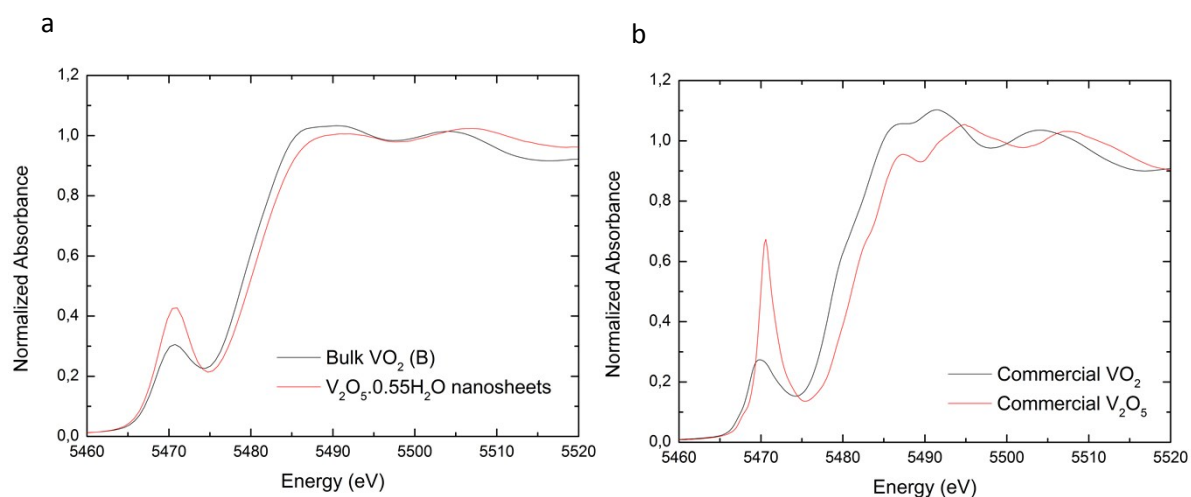


Figure S2. (a) Vanadium K-edge XANES spectra of V<sub>2</sub>O<sub>5</sub>·0.55H<sub>2</sub>O nanosheets (red line) and VO<sub>2</sub>(B) (black line); (b) Vanadium K-edge XANES spectra of standard commercial V<sub>2</sub>O<sub>5</sub> (red line) and VO<sub>2</sub> (black line).

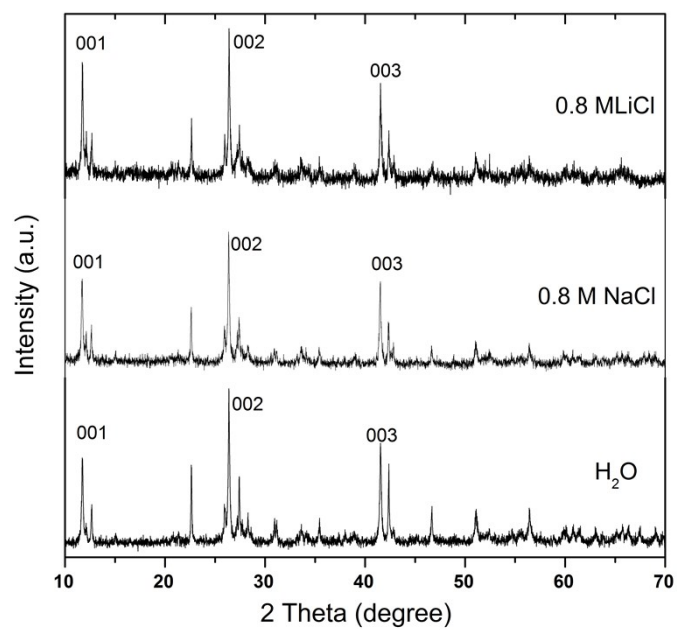


Figure S3: Powder XRD patterns for VO<sub>2</sub>(B) after refluxing for 24h at room temperature in pure deionized water, 0.8 M NaCl solution, and 0.8 M LiCl solution.

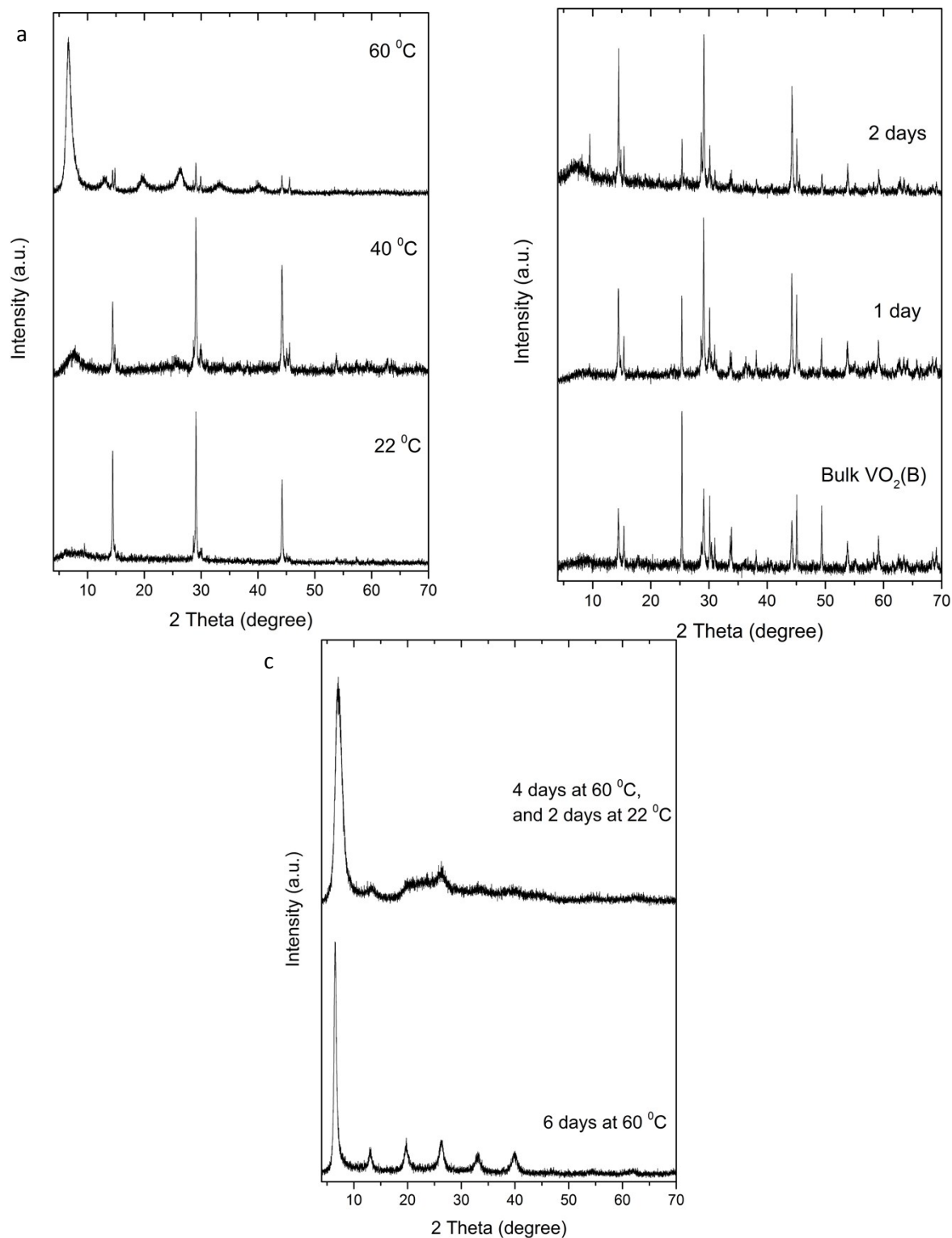


Figure S4: (a) Powder XRD patterns for VO<sub>2</sub>(B) after refluxing in water for 5 days at 22 °C, compared with that refluxed in water for the same period at 40, and 60 °C; (b) powder XRD patterns for bulk VO<sub>2</sub>(B), compared with that refluxed in water for 1 and 2 days at 60 °C; and (c) powder XRD patterns for VO<sub>2</sub>(B) after refluxing in water for 6 days at 60 °C, compared with that refluxed in water for 4 days at 60 °C and 2 days at 22 °C.

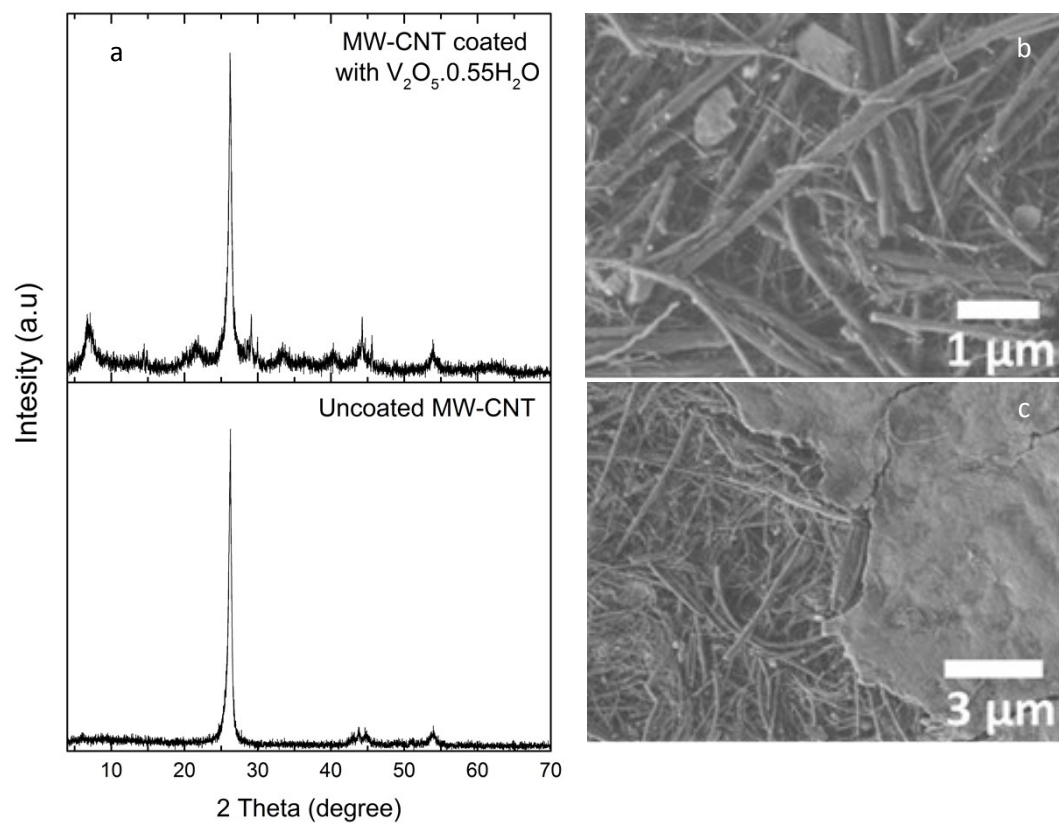


Figure S5: (a) Powder XRD pattern of uncoated MW-CNT and that coated with our exfoliated material using diluted suspension, (b) and (c) SEM images of the coated MW-CNT at different magnification. (d) SEM images of cross-section of the four electrodes used in our study.

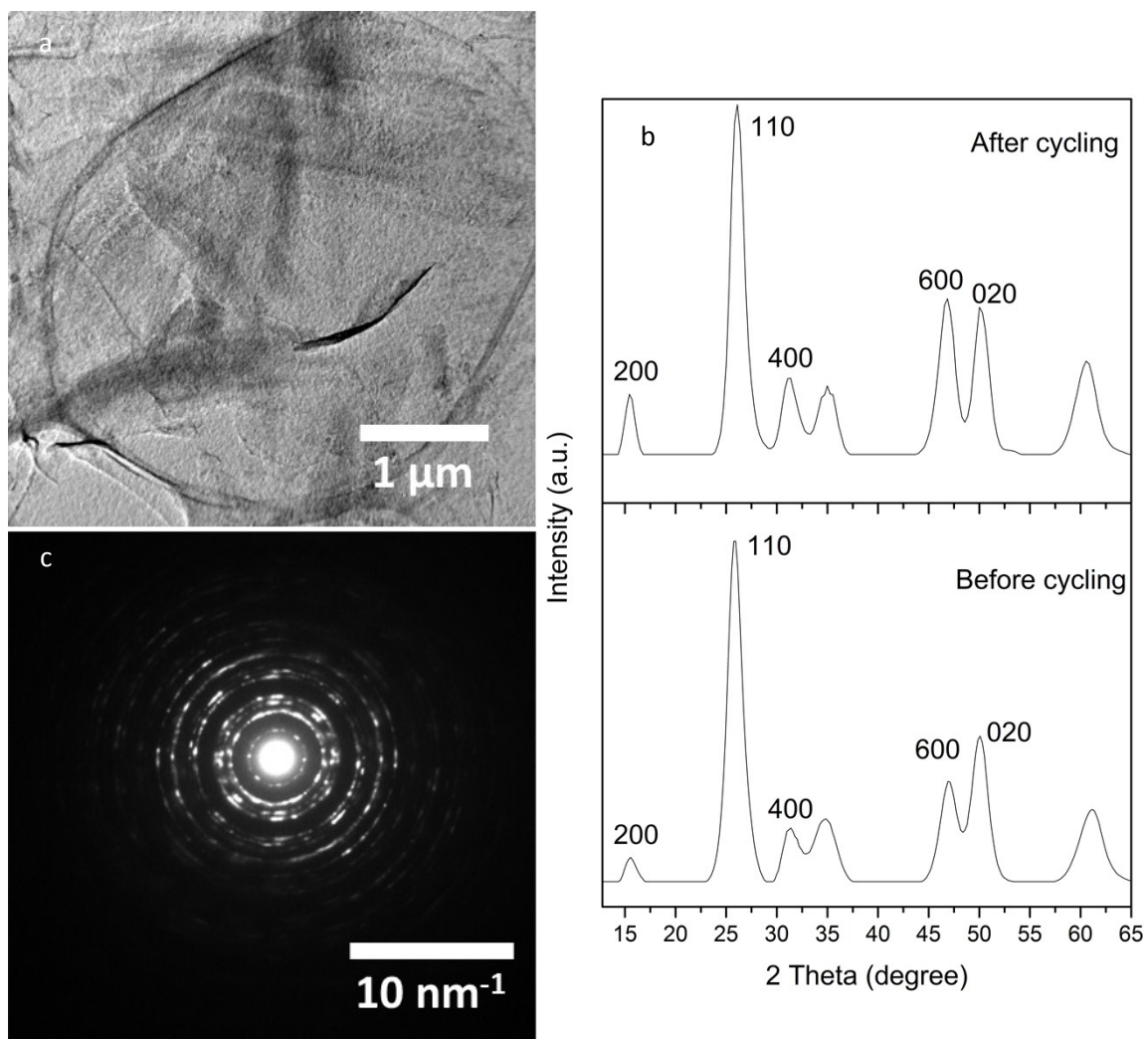


Figure S6: (a) TEM image and (b) the corresponding SAED pattern of  $V_2O_5 \cdot 0.55H_2O$  nanosheets obtained from electrode VO-45 after the electrochemical cycling for 20 cycles. (c) Simulated powder pattern obtained from the SAED pattern of  $V_2O_5 \cdot 0.55H_2O$  before and after cycling (simulation done using CRISP 2.2 program).<sup>2</sup>

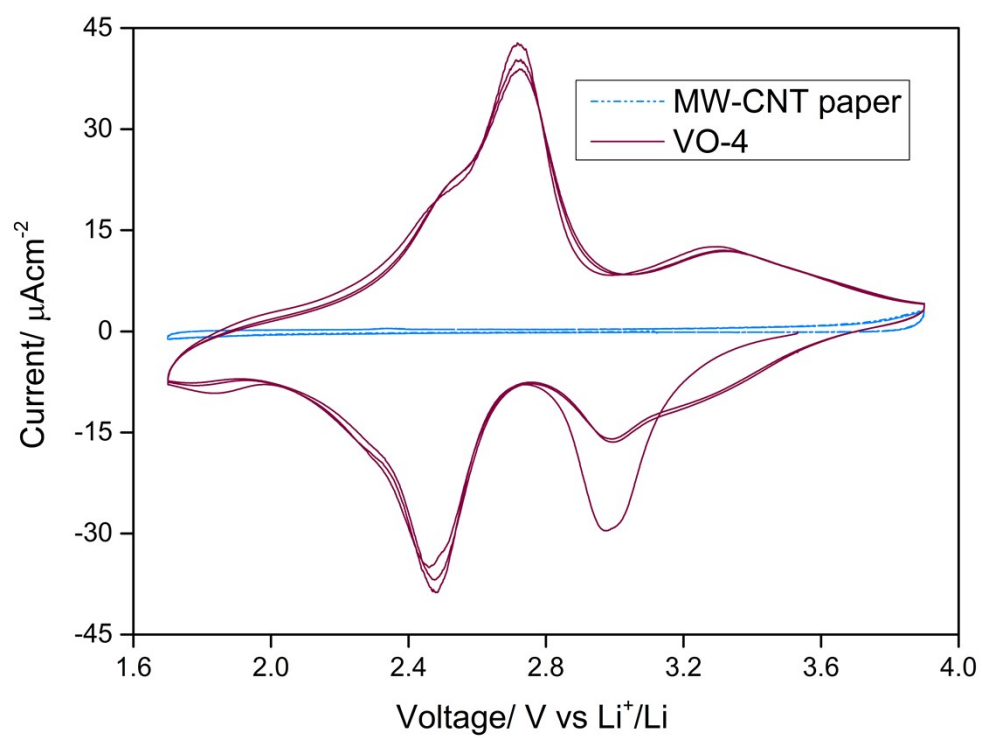


Figure S7: Cyclic voltammograms of the uncoated MW-CNT paper and electrode VO-4 (MW-CNT paper coated with the exfoliated vanadium oxide).

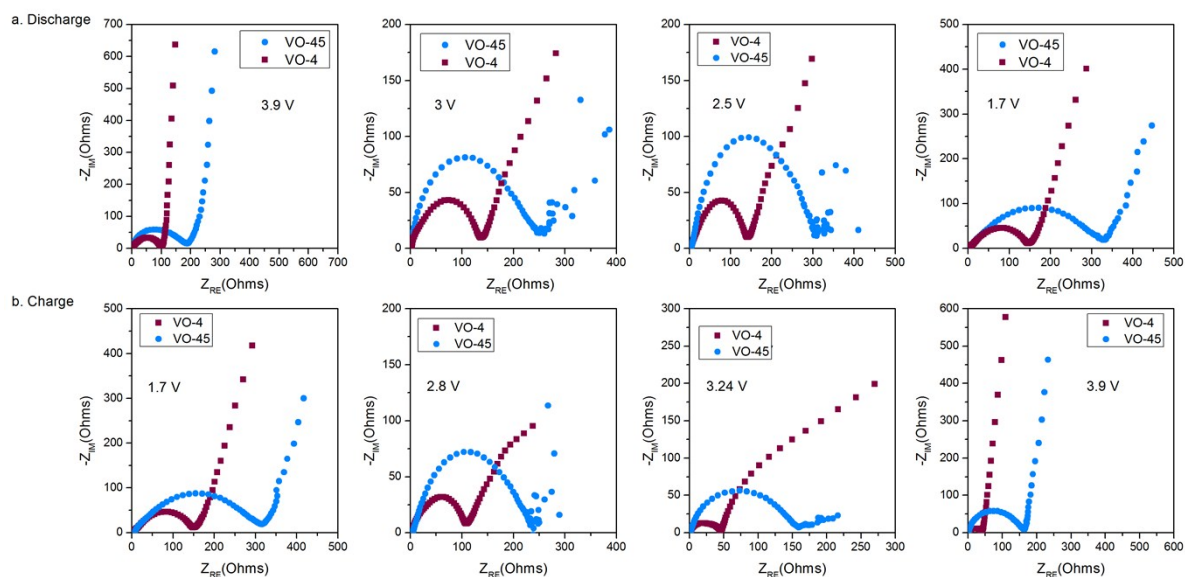


Figure S8: Electrochemical impedance spectroscopy (EIS) data collected for electrodes VO-45 and VO-4 at various voltages during discharge (a) and charge (b). The Nyquist plots shown above indicate that the electrode with a thicker oxide film (VO-45) is more resistive as compared to electrode VO-4.

Table S1: Comparison of the morphology and electrochemical performance of  $V_2O_5 \cdot nH_2O$  reported in this study and previously reported work.

Electrode Material Description	Morphology	Capacity / mAhg <sup>-1</sup>	C-rate or current density / mAg <sup>-1</sup>	Potential range / V	Reference
$V_2O_5 \cdot nH_2O$ / CNT paper	Ultrathin nanosheets	280	200	1.7-3.9	This work
$V_2O_5 \cdot nH_2O$ / CNT	Nanobelts	241	200	2.0-4.0	Xianhong Rui <i>et.al.</i> <sup>3</sup>
$V_2O_5 \cdot nH_2O$ xerogel / graphene	Ribbons	239	30	1.5–4.0	Guodong Du <i>et.al.</i> <sup>4</sup>
$V_2O_5 \cdot nH_2O$ xerogel	2D flakes composed of thin acicular nanowires	300	200	1.5–4.0	Qilong Wei <i>et.al.</i> <sup>5</sup>
$V_2O_5 \cdot nH_2O$ xerogel	Network of long ribbons	250	0.1 C	1.5-3.6	Qi Liu <i>et.al.</i> <sup>6</sup>
$V_2O_5 \cdot nH_2O$ xerogel / 2% reduced graphene oxide	Network of long ribbons	419	0.1 C	1.5-3.6	Qi Liu <i>et.al.</i> <sup>6</sup>
$V_2O_5$ aerogel	Network of ribbons	291	0.25 C	1.5-4.0	Arianna Moretti <i>et.al.</i> <sup>7</sup>

References:

- 1 L. Liu, T. Yao, X. Tan, Q. Liu, Z. Wang, D. Shen, Z. Sun, S. Wei and Y. Xie, *Small*, 2012, **8**, 3752–6.
- 2 S. Hovmöller, *Ultramicroscopy*, 1992, **41**, 121–135.
- 3 X. Rui, J. Zhu, W. Liu, H. Tan, D. Sim, C. Xu, H. Zhang, J. Ma, H. H. Hng, T. M. Lim and Q. Yan, *RSC Adv.*, 2011, **1**, 117–122.
- 4 G. Du, K. H. Seng, Z. Guo, J. Liu, W. Li, D. Jia, C. Cook, Z. Liu and H. Liu, *RSC Adv.*, 2011, **1**, 690–697.
- 5 Q. Wei, J. Liu, W. Feng, J. Sheng, X. Tian, L. He, Q. An and L. Mai, *J. Mater. Chem. A*, 2015, **3**, 8070–8075.
- 6 Q. Liu, Z.-F. Li, Y. Liu, H. Zhang, Y. Ren, C.-J. Sun, W. Lu, Y. Zhou, L. Stanciu, E. a Stach and J. Xie, *Nat. Commun.*, 2015, **6**, 6127.
- 7 A. Moretti, F. Maroni, I. Osada, F. Nobili and S. Passerini, *ChemElectroChem*, 2015, **2**, 529–537.